Hindawi Publishing Corporation
International Journal of Distributed Sensor Networks
Volume 2014, Article ID 213012, 12 pages
http://dx.doi.org/10.1155/2014/213012

Research Article

iAMCTD: Improved Adaptive Mobility of Courier Nodes in Threshold-Optimized DBR Protocol for Underwater Wireless Sensor Networks

N. Javaid,[1,2] M. R. Jafri,[2] Z. A. Khan,[3] U. Qasim,[4] T. A. Alghamdi,[5] and M. Ali[6]

[1] *CAST, COMSATS Institute of Information Technology, Islamabad 44000, Pakistan*
[2] *EE Department, COMSATS Institute of Information Technology, Islamabad 44000, Pakistan*
[3] *Internetworking Program, FE, Dalhousie University, Halifax, NS, Canada B3J 4R2*
[4] *University of Alberta, AB, Canada T6G 2J8*
[5] *CS Department, College of CIS, Umm AlQura University, Makkah 21955, Saudi Arabia*
[6] *Institute of Management Sciences, Peshawar 25000, Pakistan*

Correspondence should be addressed to N. Javaid; nadeemjavaid@comsats.edu.pk

Received 10 February 2014; Accepted 2 June 2014; Published 20 July 2014

Academic Editor: Aneel Rahim

We propose forwarding-function (F_F) based routing protocol for underwater sensor networks (UWSNs): improved adaptive mobility of courier nodes in threshold-optimized depth-based-routing (iAMCTD). Unlike existing depth-based acoustic protocols, the proposed protocol exploits network density for time-critical applications. In order to tackle flooding, path loss, and propagation latency, we calculate optimal holding time (H_T) and use routing metrics: localization-free signal-to-noise ratio (LSNR), signal quality index (SQI), energy cost function (ECF), and depth-dependent function (DDF). Our proposal provides on-demand routing by formulating hard threshold (H_{th}), soft threshold (S_{th}), and prime energy limit (R_{prime}). Simulation results verify effectiveness and efficiency of the proposed iAMCTD.

1. Background

Underwater acoustic sensor networks (UASNs), as a subclass of wireless sensor networks (WSNs), are specifically used for monitoring purposes in aqueous environment. The acoustic wireless sensors along with sink(s), distributed under water, constitute the basic body of UASN, where acoustic sensors gather the information of interest and then following a routing strategy forward these data to the end station. WHOI Micro-Modem [1] and Crossbow Mica2 [2] are among the commercially available sensors for underwater environments. Sink is generally supposed to have no power constraint, whereas the acoustic sensors are equipped with limited battery power. These networks provide diversified range of applications like pollution monitoring, ocean current detection, submarine discovery, deep sea explorations, and seabed management.

Due to the nature of aqueous environment, improving energy efficiency at routing layer is a challenging task. Moreover, as there are major differences between terrestrial and underwater conditions, hence the basic concepts of terrestrial routing can not be implemented in UWSNs. To tackle these problems, researchers exercise the role of low speed acoustic signals for aqueous communication and sea navigation systems, leading to high propagation delay and transmission losses. High shipping activity, thermal noise, and turbulent noise also increase the error rate. Authors in [3] design the underwater acoustic channel to descriptively analyze the total noise density and path loss. On the other hand [4], it investigates diverse routing architectures for 2-dimensional and 3-dimensional UWSNs. Fundamental analyses of aqueous conditions show that reactive routing is more challenging than the proactive one. Battery replacement and efficient routing are among the solutions to overcome the

power constrained problem of acoustic sensors; however, the leading solution is not practical; thereby, we focus on the lagging one.

The two major categories of underwater routing protocols are localization-based and localization-free. The fundamental difference between these two is the awareness of location by the sensor nodes. Localization-free protocols are also termed as flooding based schemes, where nodes are only aware about their depth. On the other hand, location-based protocols assume that the sensor nodes are location aware. In literature, both localization-based and localization-free schemes are available: QELAR [5], R-ERP2R [6], EEDBR [7], and MPT [8]. These protocols attempt to tackle high transmission delay, path loss, and receiving energy consumption. However, deficiencies do exist. Depth Based Routing (DBR) protocol [9] is based on depth of sensor nodes as the trivial parameter in flooding-based forwarding schemes. EEDBR [7] improves the deficiencies of DBR by considering residual energy while selecting data forwarder(s). R-ERP2R [6] is another magnificent depth-based routing scheme, which implements "ETX" routing metric for improving energy efficiency. QELAR [5] designs routing architecture and cross-layer approach on the basis of Q-machine learning, thereby improving localization-based routing. MPT [8] employs power-controlled and source-initiated transmission by examining the deficiencies at the physical layer in UASNs, specifically to deal with on-demand applications. H2-DAB [10] achieves the minimum delay and higher network lifetime by using hop count as routing metric. It also employs courier nodes to provide adaptability for time-critical and data-sensitive applications.

There is always a need of less complex and highly reliable communication scheme in WSNs and UWSNs. Liu et al. [11] improve reliability in transmissions by proposing a network coding based cooperative communications scheme (NCCC). It provides a scalable implementation of NCCC by selecting coding vectors from finite field. Localization schemes for sensor nodes are not so accurate in UWSN, as in WSN. In WSN, mobile beacon assisted localization is used.

In [12], the authors propose Z-curve, which is a path planing mechanism for mobile beacons to localize the sensor nodes. Zou et al. [13] develop a generic algorithm to control the movement of autonomous underwater vehicles (AUVs) in UWSN by gathering network information from sensor nodes. Limited residual energy is one of the main challenges for sensor nodes in UWSN. High numbers of (re)transmissions and collisions cause consumption of energy. In [14], the authors tackle the issue by proposing contention-free multichannel MAC protocol for UWSNs.

Another technique has been proposed by [15] in which authors design spatially fair MAC (SFMAC) protocol for UWSNs. It avoids the collisions with postponing clear-to-send (CTS) for a specific duration as calculated by the receiver node. Mobility of the target object is always an issue for WSN. Furthermore, it is very difficult to update the location information of the target object by sensor nodes. In [16]; the authors suggest an accurate target tracking scheme for WSNs. They achieve energy efficiency in the scheme by minimizing the missing rate of an object.

MUAP in [17] examines the acoustic channel as well as its losses and then proposes an energy model for the computation of channel losses in aqueous environment. Stojanovic [18] carefully examines the association between transmission distance and channel capacity in underwater communication. CEDC [19] uses doppler compensation model to improve the scrutinizing of acoustic signals and present a high data-rate communication model. In dense underwater conditions, PULRP [20] provides a cross-layer model as well as a descriptive algorithm to maximize network's throughput. This model is localization-free technique with efficient energy consumption model. AMCTD [21] exploits the adaptive mobility of courier nodes to maximize the network lifetime. It computes the holding time on the basis of weight function to cope with the problems of high transmission loss and low network lifetime. The work presented in this paper is the extension of [21].

2. Motivation and Contribution

By examining the flooding as well as depth-based routing protocols, we compensate for the deficiencies in these schemes. In DBR and EEDBR, stability period quickly ends due to unnecessary data forwarding and high load on low-depth nodes. Another main deficiency of these protocols is a sharp instability period due to the quick energy consumption of medium-depth nodes. In AMCTD, the high transmission loss is due to distant transmissions of medium-depth nodes. AMCTD is not suitable for data-sensitive applications, especially during instability period due to the mobility pattern of courier nodes. The consideration of only two parameters, depth and residual energy, is not sufficient for global load balancing throughout the network lifetime.

We investigate the problems of medium-depth nodes in the earlier rounds like high end-to-end delay and transmission loss, low stability period, and fast energy consumption. Based on these, we optimize the movement of courier nodes in sparse conditions for load balancing. Although AMCTD's performance is better than DBR and EEDBR, respectively; however, deficiencies do exist. We try to overcome the deficiencies as follows.

(i) In iAMCTD, the efficient movement of courier nodes minimizes end-to-end delay and decreases the energy consumption of low-depth nodes in sparse conditions.

(ii) The F_{Fs} computation technique causes longer stability period than the previous ones along with reduced transmission loss. It also decreases average end-to-end delay of packets which is crucial for time-critical applications.

(iii) Implementation of threshold-optimized data forwarding is resourceful process for on-demand routing and removes forwarding of unnecessary data in the network.

(iv) Optimized mobility pattern of sink, in later rounds, maintains end-to-end delay of the network, especially

for delay-sensitive applications even in sparse conditions.

(v) We examine nodes' depth and control overhead at physical layer as well as network layer and propose a model which caters for the major acoustic problems.

We consider arbitrary deployment of nodes in 3D aqueous environment. The network consists of sensor nodes, courier nodes, multiple sinks, and onshore data centers. Sensor nodes and courier nodes communicate with low-range acoustic modems, whereas sinks (equipped with both RF and acoustic modems) communicate with onshore data centers and sensor nodes. Upon the detection of physical environmental attributes, the sensor nodes transmit the sensed data to either of the in-range node or sink. Courier nodes are equipped with mechanical modules for movement control; however, these can only relay the network data towards sink. After collecting threshold-based data, sensor nodes transfer the data to sink, as soon as possible, either by direct transmission or through courier nodes; otherwise they broadcast the data towards their neighbors. Nodes communicate with each other using low-range commercial acoustic modems. In flooding-based techniques, control packets' transmission is the requirement of network in order to achieve better management with the varying network density. The multiple-sink model is proficient at balancing the network load and it has been analyzed in [22–24].

3. The Proposed iAMCTD

We divide operation of the proposed iAMCTD into the following four phases:

(i) network initialization and underwater channel model,

(ii) implementation of on-demand data routing,

(iii) data forwarding phase,

(iv) adaptive mobility patterns of courier nodes.

The first phase deals with nodes' deployment, network initialization, and thorp's model [18] for path loss and noise density calculation in aqueous environment. Second phase discusses implementation of on-demand data routing to facilitate the time-sensitive and critical-data applications. Third phase expresses the data forwarding along with the variations in depth thresholds for sensor nodes to cope with varying network density. We develop efficient forwarding functions for optimal data forwarding in aqueous environment. We also discuss the data packet structure and the tradeoff between control overhead and network lifetime. On the basis of control packets, sink identifies the network density and manages the network specifications and mobility of courier nodes. Last phase uses mixed integer linear programming (MILP) to analyze adaptive mobility patterns of courier nodes and their multiple cases.

3.1. Network Initialization and Underwater Channel Model. We assume that sensor nodes broadcast the data using flooding-based approach. As each neighbor of the node receives data of the sender node, courier nodes devise their sojourn tour at the start of the network and then start collecting data from the source nodes. These also report the network density information to sinks in order to devise mobility patterns and depth-threshold variations. During knowledge acquisition, nodes share the depth and residual energy information among themselves. As the network initiates, courier nodes remain at equal horizontal distances from each other and these start vertical movement towards the bottom.

Given below channel model is used to calculate spreading loss and total noise loss in underwater acoustics. We calculate the total attenuation of signal on the bases of spreading loss [3] and thorps model for signal absorption loss. At a given frequency f, the channel model calculates absorption loss $\alpha(f)$ [18] as follows:

$$10\log(\alpha(f)) = \begin{cases} \dfrac{0.11f^2}{(1+f^2)} + \dfrac{44f^2}{(4100+f)} + 2.75 * 104f^2 + 0.003 & f \geq 0.4 \\ 0.002 + 0.11\left(\dfrac{f}{(1+f)}\right) + 0.011f, & f < 0.4, \end{cases} \quad (1)$$

where $\alpha(f)$ is measured in dB/km and f in kHz. Here, thorps model defines formula for the calculation of absorption loss. By using the value of absorption loss, we calculate the value of α as follows:

$$\alpha = \frac{10^{\alpha(f)}}{10}. \quad (2)$$

Accordingly, all tunable parameters are given in *dBreμPa*. Combining absorption loss and spreading loss, the total attenuation $A(l, f)$ can be computed as follows:

$$10\log(A(l,f)) = k * 10\log(l) + l * 10\log(\alpha(f)), \quad (3)$$

where the first term denotes spreading loss and the second term is the absorption loss. The spreading coefficient k defines the geometry of the signal propagation in underwater acoustics (i.e., $k = 1$ for cylindrical, $k = 2$ for spherical, and $k = 1.5$ for practical spreading [25]). For the calculation of ambient noise in underwater networks, total noise is comprised of four main parts: turbulent noise, shipping noise, wind noise, and thermal noise. The following formulae give the power spectral density [3] of the four noise components in *dBreμPa*, as a function of f in kHz:

$$10\log(N_t(f)) = 17 - 30\log(f),$$

$$10\log(N_s(f)) = 40 + 20(s - 0.5) + 26\log(f) - 60\log(f + 0.03),$$

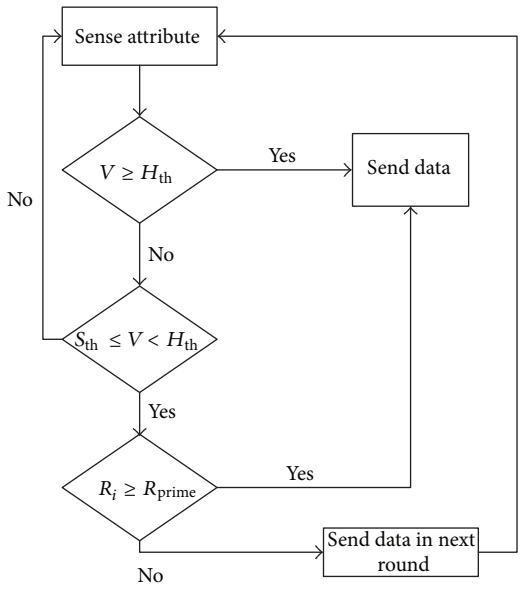

Figure 1: Routing of on-demand data.

$$10\log\left(N_w\left(f\right)\right) = 50 + 7.5w^{1/2} + 20\log\left(f\right) - 40\log\left(f + 0.4\right),$$
$$10\log\left(N_{\text{th}}\left(f\right)\right) = -15 + 20\log\left(f\right), \tag{4}$$

where N_t, N_s, N_w, and N_{th} represent the noise due to turbulence, shipping, wind, and thermal activities respectively. The overall noise power spectral density is calculated as

$$N\left(f\right) = N_t\left(f\right) + N_s\left(f\right) + N_w\left(f\right) + N_{\text{th}}\left(f\right). \tag{5}$$

The flooding-based approaches employ receiver-based data forwarding due to un-awareness of location. Each node shares depth information with other nodes and the eligible neighbors for forwarding are decided on the basis of depth threshold. The neighbor nodes compute the forwarding functions by considering channel losses, residual energy, and depth differences.

3.2. Implementation of On-Demand Data Routing. The proposed protocol performs on-demand data routing as the nodes react immediately to sudden and drastic changes considering the value of sensed attribute. Figure 1 depicts the transmission algorithm for threshold-based data.

Where V is the current sensed value, S_{th} is the soft threshold, H_{th} is the hard threshold, R_i is the residual energy of the ith node, and R_{prime} is the residual energy limit for data transmission. After sensing the attribute value, each node compares it with the hard threshold. If it finds the value above than H_{th}, then immediately it sends the data. Else, if the value is between H_{th} and S_{th}, it compares its residual energy with R_{prime}; if the residual energy is greater than R_{prime}, it transmits data towards sink; otherwise it waits for the next round. For temperature sensing applications, we assume H_{th} as 30°C, S_{th} as 20°C, and R_{prime} as 40 Joules. We analyze that traditional techniques consume surplus energy in two cases: transmission of redundant data and retransmission of sensitive data. We exploit receiver based forwarding and minimize the transmission of normal data messages in number; the transmission energy loss is minimized. We also apply power control strategies at physical layer to avoid aqueous channel losses preventing critical data loss.

Sender ID	Packet sequence number	Depth	Payload...

Figure 2: Data packet format.

3.3. Data Forwarding Phase. The sensor nodes send sensed data to in-range courier node(s). Upon reception, the courier node(s) acknowledge the sender node(s) to reduce further flooding. In the absence of courier nodes, sensor node sends data towards their neighbor nodes. Each sensor node calculates holding time for received packet on the basis of forwarding function. In order to avoid packet collisions, all nodes maintain a timer to send threshold-based sensitive data. Nodes sense packets buffer and maintain priority queue to avoid transmission of same data and to forward packets on the basis of holding time. Thus, the end-to-end delay of critical data decreases, increasing network's feasibility for time sensitive applications. The sensor nodes, after every 100 rounds, transmit control packets for the computation of network density at the sink, which is further utilized to manage the variation in the mobility patterns of courier nodes and depth-thresholds. The data packet format of our technique is shown in Figure 2 which consists of sender ID, packet sequence number, depth information, and payload.

The trade-off between control overhead and network lifetime is a serious consideration in the design of flooding-based routing techniques, so we attempt to control this trade-off by employing minimal overhead.

3.3.1. Variation in Depth Threshold. In preceding depth-based schemes, nonvarying depth-threshold is another key reason of flooding in dense situations. It is also due to the absence of eligible neighbors in sparse conditions specifically during instability period, which causes the loss of critical data. Therefore, we implement variations in depth-threshold of nodes according to network density. The three optimal values for depth thresholds are D_{th1}, D_{th2}, and D_{th3}, which are calculated by the base station in the network according to the number of dead nodes in the network. In Figure 3, ε_1 and ε_2 are the limits for the implementation of thresholds.

With a network of 225 nodes and each nodes' range 100 m, we assume the values of D_{th1}, D_{th2}, and D_{th3} as 60 m, 40 m, and 20 m, and ε_1 and ε_2 are set as 5 and 150, respectively.

3.3.2. Forwarding Function Computation. In this section, we analytically model the optimal value selection for F_F. There are three types of main F_F: signal quality index (SQI),

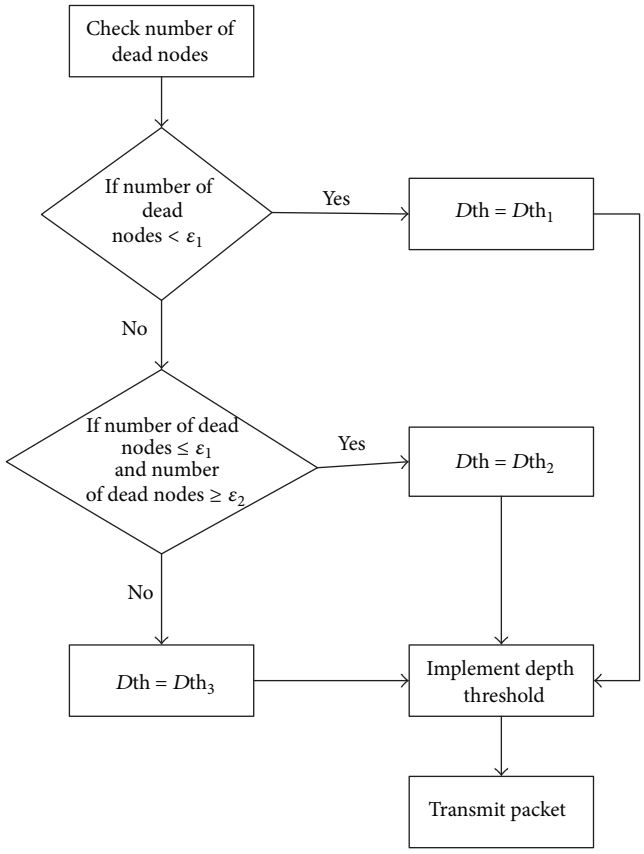

Figure 3: Variations in depth threshold.

energy cost function (ECF), and depth dependent function (DDF). As sensor node sends data, the neighbor node having highest F_F has least holding time; hence, the optimal forwarder will be selected. Sensor nodes select the F_F on the basis of depth information. For a specific region (low-depth, medium-depth, high-depth), appropriate type of F_F is selected on the bases of residual energy, SNR ratio, and depth differences between sender and receiver. The mechanism for the implementation of F_F is given in Figure 4.

Where, D_1 and D_2 are depth-distributions, and are assumed 150 m and 350 m, respectively, in the region of depth 500 m. F_F formulation considers the overall conditions of aqueous environment. The upper region of water has maximum interference, noise, and shipping activity; hence the SQI prioritizes SNR to achieve minimal transmission loss of the signal.

In medium-depth region, load on nodes is high due to frequent data forwarding, so the ECF grants the significance of residual energy of nodes to attain global load balancing in the network. In last region, we formulate DDF to accomplish distant forwarding and minimum flooding scenarios. The formulae for these functions and holding time H_T calculation are given below:

$$H_T = \left(1 - F_F\right) H_{t\max}, \tag{6}$$

where $H_{t\max}$ is the maximum holding time and can be selected according to environmental conditions. In depth-based techniques, sensor nodes are not mindful of their location but only of their depth. Therefore, we define localization-free signal-to-noise ratio LSNR based on the notion of SNR [3] to assess transmission loss of the signal between two nodes. In addition, we introduce SQI as a routing metric on the basis of LSNR in low-depth acoustic region. LSNR is computed on the basis of $A(l, f)$ which considers depth difference l instead of euclidean distance d, as the receiver can only compute the depth difference with the sender node:

$$\text{LSNR} = \frac{P_t}{\left(A\left(l, f\right) N\left(f\right)\right)}, \tag{7}$$

where P_t is the constant transmitted power. Attenuation noise (AN factor) is the product of path loss and ambient noise. f indicates the frequency of the signal in kHz. By applying LSNR, SQI is calculated as

$$\text{SQI} = \frac{\left(\text{LSNR}\left(R_i\right)\right)}{l_i}, \tag{8}$$

where R_i denotes the residual energy of ith receiver node and l_i is the depth difference between sender and the receiver nodes. Figure 5 demonstrates the overall data forwarding mechanism of iAMCTD. In medium-depth region, the nodes are burdened due to maximum packet forwarding. Their energy depletes earlier than the others, causing network instability and loss of critical data (received from high-depth nodes). Therefore, it is a major requirement to consider the residual energy of nodes while selecting optimal forwarder(s). We compute ECF in such a manner that it prioritizes both residual energy and depth of receiver nodes:

$$\text{ECF} = \frac{\text{priority}_{\text{value}}\left(R_i\right)}{D_i}, \tag{9}$$

where D_i is the depth of the sensor node and $\text{priority}_{\text{value}}$ is a constant which can be adjusted according to stability requirement. In the last region, the channel losses are not so high; however, forwarding load is higher than the other regions; therefore, courier nodes help to reduce load on these nodes to acquire network stability. High-depth region of aqueous environment has high interference due to aqueous noises, sea life, and mineral density. In order to deal with these problems, we formulate DDF prioritizing both residual energy and SQI of received signal, expressed as

$$\text{DDF} = \frac{\left(\text{SQI} \times l_i\right)}{D_i}. \tag{10}$$

In receiver-based forwarding, multiple nodes choose the optimal forwarder between themselves. It is also important to decrease the flooding mechanism during forwarding. Multiple transmissions of same data cause higher average energy consumption by the network than by other interferences. So, it is necessary to cope with it. A simple algorithm for data forwarding using F_F is given in Algorithm 1.

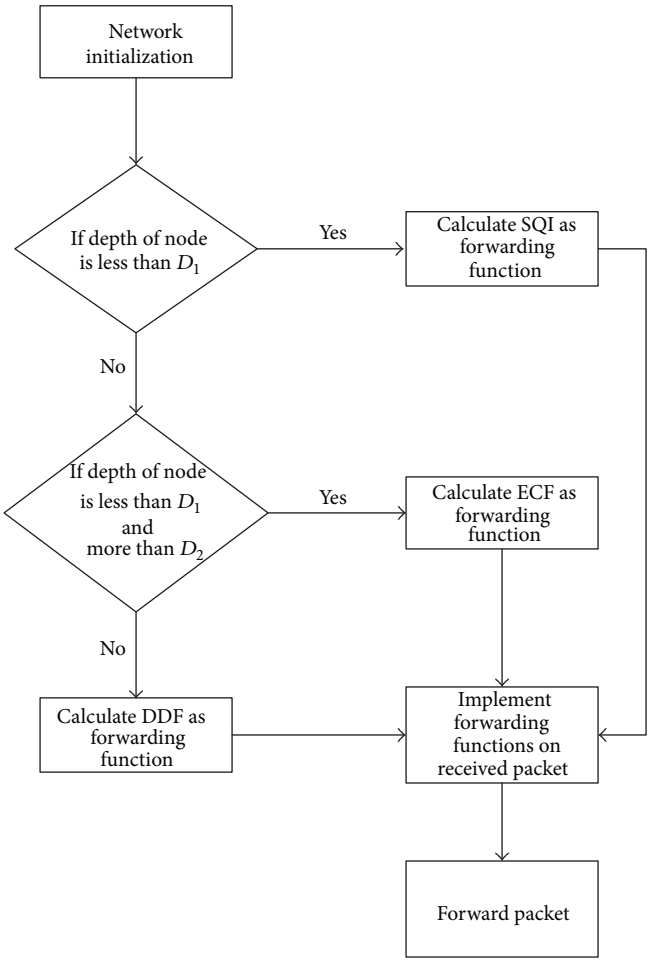

Figure 4: Analytical model for data forwarding.

3.4. Adaptive Mobility Patterns of Courier Nodes. Courier nodes are highly resourceful in stabilizing network condition as these collect data from sensor nodes by their adaptive mobility. After network initialization, courier nodes start their movement towards the bottom of network along with collecting data from the nodes in their vicinity. Thus, reduce the load on medium-depth nodes by acting as a relay(s) and then receive data from high-depth nodes, an efficient approach for time-critical applications. Furthermore, courier nodes change the mobility pattern as network density (controlled by BS) varies. These nodes maintain the depth and vertical movement by using mechanical module [10].

3.4.1. Aggregate Traffic Model for Mobile Courier Nodes. We propose Aggregate-Traffic-Model (ATM) and formulate the objective functions to achieve higher throughput by utilizing adaptive mobility patterns of courier nodes.

In the proposed mobility pattern, we are interested in maximizing the total information flow towards the sink by all courier nodes, that is,

$$\text{Maximize} \quad I \tag{11}$$

$$\text{subject to :} \quad \sum_{y} I_y \geq I \quad \forall y \tag{12}$$

$$\sum_{j} \sum_{i=1}^{k} a_{i,j}^{y} \geq I_y \quad \forall j, y \tag{13}$$

$$\sum_{i=1}^{k} a_{i,j}^{y} \geq I_j^{y} \quad \forall j, y \tag{14}$$

$$I_{y,o} - I_{o,y} \geq 0 \tag{15}$$

$$x_{i,j} = \{0, 1\} \quad \forall i, j \tag{16}$$

$$x_{j,o} = \{0, 1\} \quad \forall j \tag{17}$$

$$T_s = \sum_{u} \tau_u \quad \forall u \tag{18}$$

$$0 \leq \tau_u \leq \tau_{\max} \quad \forall u \tag{19}$$

$$l \leq 2d. \tag{20}$$

Equation (11) defines the objective function: maximize the total information flow towards the sink. Equation (12) ensures that the total information flow towards sink from courier node y will not surpass the sum of information flows of all couriers nodes towards sink. Equation (13) describes that I_y is less than or equal to the sum of information flows

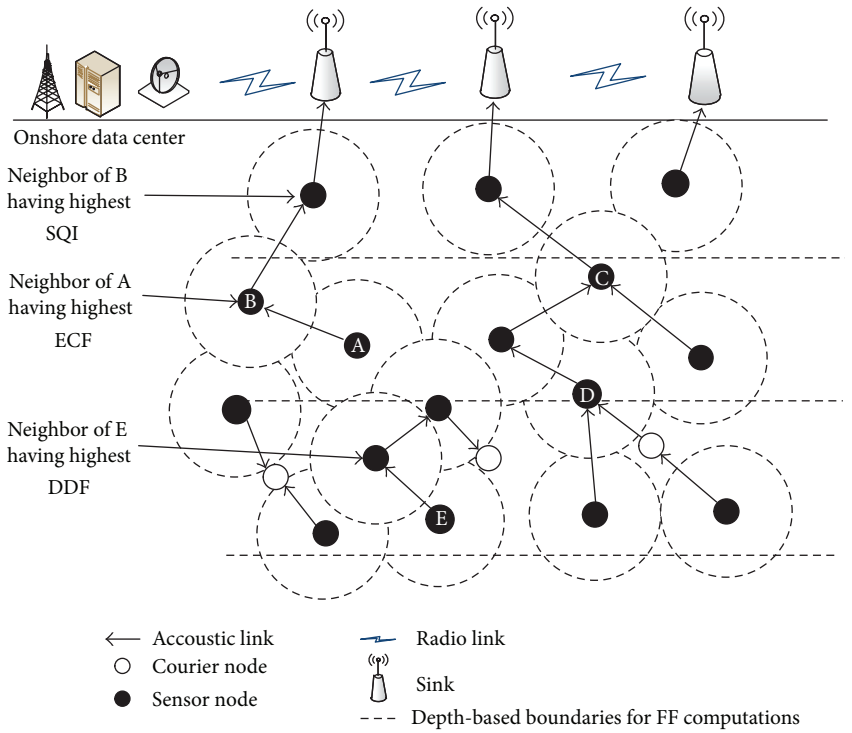

Figure 5: Mechanism of data transmission in iAMCTD.

$D_1 \leftarrow$ Upper limit for depth
$D_2 \leftarrow$ Lower limit for depth
$D_i \leftarrow$ Depth of ith node
$\text{SQI}_i \leftarrow$ Signal Quality Index of ith node
$\text{ECF}_i \leftarrow$ Energy Cost Function of ith node
$\text{DDF}_i \leftarrow$ Depth Dependent Function of ith node
$F_{Fi} \leftarrow$ Forwarding Function of node i
if $D_i \leq D_1$ **then**
  $F_{Fi} = \text{SQI}_i$
else $\{D_1 < D_i \leq D_2\}$
  $F_{Fi} = \text{ECF}_i$
else
  $F_{Fi} = \text{DDF}_i$
end if

Algorithm 1: Data forwarding mechanism.

from all descendent nodes in its one sojourn tour at different sojourn locations, where j shows the sojourn location of the yth courier node. Equation (14) deals with flow conservation at sojourn location of the courier node. Equation (15) shows flow conservation between any courier node and sink, where o is the location of sink. Equations (16) and (17) ensure the presence of courier nodes in the vicinity of sensor nodes and sink, respectively, where "1" shows the presence and "0" shows the absence of courier node(s). By providing the upper bound $\tau_{\max}$, (18) and (19) limit the total sojourn time of any courier node in one sojourn tour and the sojourn time at any particular sojourn location, where u denotes the duration at any particular sojourn location. Furthermore, (20) implies distance-constrained and delay-bounded mobility model by employing $2d$ to limit the total distance covered by a courier node in one sojourn tour. Under these constraints, we suggest two mobility patterns for courier nodes (refer to Figure 6).

Figure 6 illustrates the two specific mobility patterns of courier nodes. They also provide support to nodes with no neighbors in the later rounds, which efficiently deals with instability period. After receiving packets in each round, they broadcast the received packet sequence number(s) to reduce flooding.

Figure 6 shows that if the number of alive nodes is greater than β_1, then courier nodes follow the second pattern in which they are at equal horizontal distances from each other.

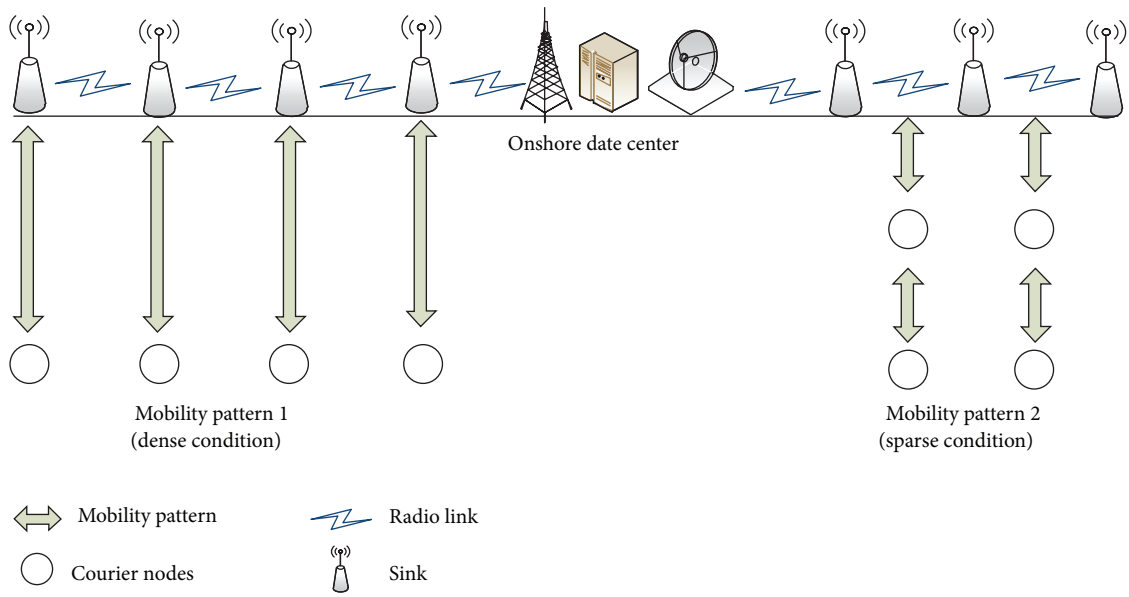

Figure 6: Adaptive mobility pattern in dense and sparse conditions.

If the number of alive nodes is less than or equal to β_1 then these follow the first pattern in which the courier nodes are in the same horizontal distance. In sparse conditions, it causes minimum end-to-end delay for remaining nodes. In pollution monitoring application, we assume β_1 as 200, β_2 as 100, and the horizontal distance between the courier nodes as 100 m to idealize the real scenario of underwater acoustics.

4. Performance Evaluation

To evaluate the performance of iAMCTD, we compare it with the selected existing schemes with the extensive simulations. Following multiple-sink model of conventional methods, we randomly deploy 225 nodes in the network field along with 4 courier nodes. We assume 100 m as nodes' transmission range and LinkQuest UWM1000 [26] as the acoustic modem(s) having 10 kbps bit rate. Moreover, the power consumptions in sending, receiving, and idle mode are 2 W, 0.1 W, and 10 mW, respectively. The size of data packets is 50 bytes and the size of control packet is 8 bytes. We implement 802.11-DYNAV [27] protocol as a core media access control protocol. Nodes are initially equipped with 70 J and hello packets are exchanged after every 100th round. In each round, all alive nodes transmit threshold-based data towards sink. After every 100th round, courier nodes compute and then report the network density to sink which supervises the depth thresholds and the adaptive mobility of courier nodes. Moreover, variations in depth threshold make our proposed scheme a feasible contender for time-critical applications such as submarine detection and tsunami detection. After network initialization, the courier nodes start moving downward from the surface of water with a mutual distance of 100 m between them.

The proposed and the existing protocols are evaluated in terms of the following performance metrics.

(i) Network lifetime: duration between network initialization and complete energy exhaustion of all the nodes.

(ii) Average energy consumption: it is the average energy consumption of all active nodes in one round.

(iii) End-to-end delay: it is the duration for a packet to be transmitted from source to destination.

(iv) Number of dead nodes: it shows the number of nodes having no energy.

(v) Transmission loss: it shows the average transmission loss (dB) between source node and sink in one round.

Figure 7 illustrates that our scheme improves the stability period of network by avoiding the forwarding of unnecessary data along with maintaining lower transmission loss. It reduces end-to-end delay by utilizing LSNR and DDF in extreme low-depth and high-depth regions, thus providing flexibility for delay-sensitive applications in UWSN. In iAMCTD, the instability period starts from almost 9000th round, after which the transmission loss (Figure 11) remains even; however, end-to-end delay (Figure 12) decreases very slowly.

Due to prioritization of SQI in the upper region, load balancing is achieved. Moreover, the load on medium-depth nodes is shared because of the adaptive movement of courier nodes. After the expiry of initial nodes, the network destabilizes due to diminution of eligible neighbors. In EEDBR, the stability period is greater than DBR; however, the network energy consumption is greater. In DBR, the stability period is lesser than the other techniques as it considers only depth of forwarding nodes as the ultimate determining factor; however, the instability period is much better than EEDBR as there is gradual increase in network energy consumption. When the network becomes sparse, number of neighbors decreases quickly causing network instability. In AMCTD,

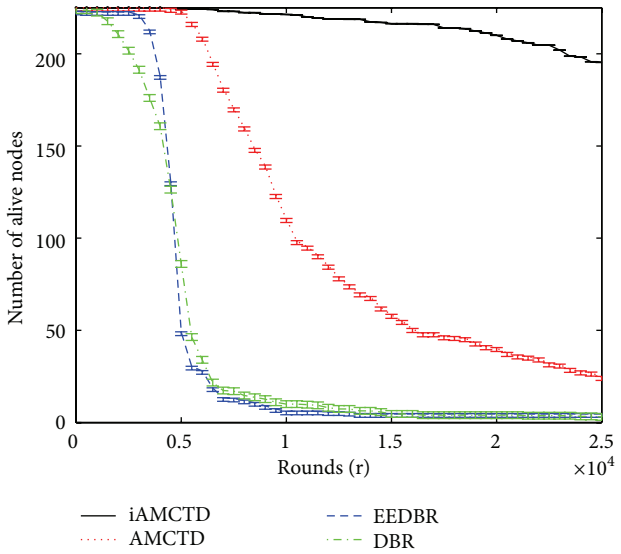

Figure 7: Number of alive nodes in iAMCTD, AMCTD, EEDBR, and DBR.

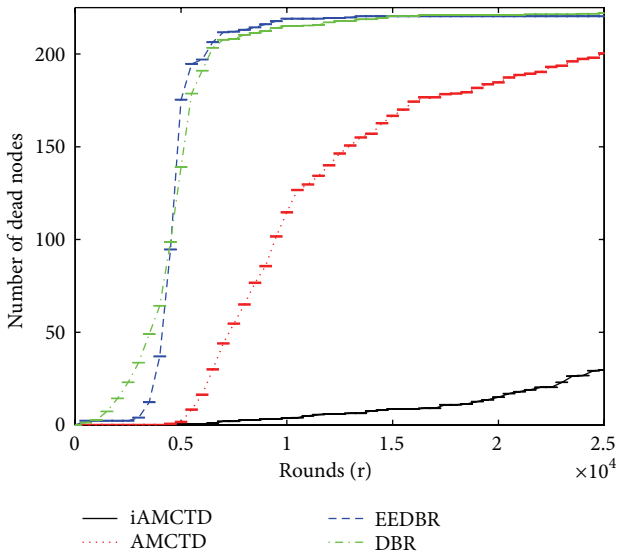

Figure 8: Number of dead nodes in iAMCTD, AMCTD, EEDBR, and DBR.

there are only two forwarding selection attributes; depth and residual energy. This consideration causes a trade-off between the network lifetime and transmission loss which is not suitable for reactive applications. The load on high-depth nodes becomes low due to the existence of courier nodes in stability period causing load balancing in AMCTD. During the instability period of AMCTD, network gradually becomes sparse causing load on high residual-energy nodes, whereas the number of neighbors is managed by variations in depth threshold. Lifetime of iAMCTD is increased due to lower throughput by responsive network. Moreover, it provides minimum transmission loss and delay which is specifically suitable for time-decisive applications such as pollution monitoring.

In our suggested scheme, employment of Thorp's energy model specifies the detailed channel losses, which are useful for selective data forwarding in responsive networks. Increase in stability period also confirms reduction in redundant transmissions.

Figure 8 shows the comparison of dead nodes in iAMCTD, AMCTD, EEDBR, and DBR. The confidence interval of results verifies that iAMCTD has almost 5000 more rounds of stability period than AMCTD due to better F_{Fs} and mobility of courier nodes, which discourages multihop forwarding. Number of dead nodes sharply increases in EEDBR as there is high load on the nodes. In DBR, low-depth nodes die at an earlier stage due to high data forwarding rate and constant depth threshold. It neglects residual energy of nodes as well as SNR. Thus, badly affecting network's throughput.

To balance load on nodes, iAMCTD selects forwarders on the bases of SNR, depth, and depth differences. Thus, preventing the creation of coverage holes which is to converse the previous techniques. Main reason behind better stability period is the implementation of efficient F_{Fs} and removal of unnecessary data forwarding in network. We conclude

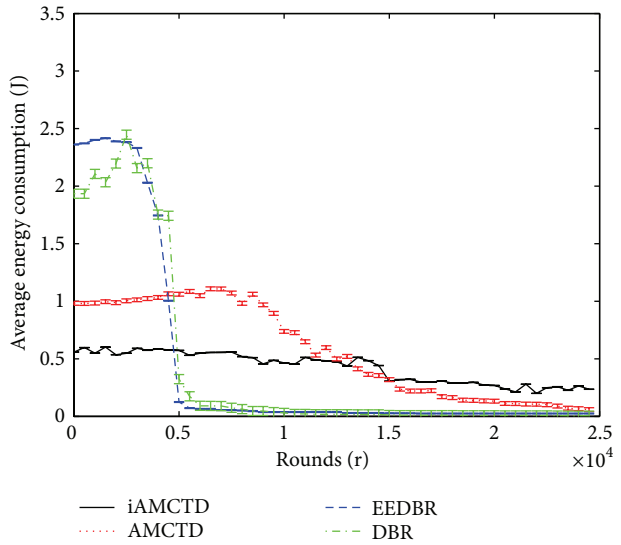

Figure 9: Total energy consumption in iAMCTD, AMCTD, EEDBR, and DBR.

that none of the proactive routing protocols are acceptable in delay-sensitive underwater applications. Furthermore, proactive routing is more expensive and less competent than on-demand routing in rapidly varying underwater environments.

Figure 9 shows that iAMCTD consumes almost constant energy throughout the network lifetime as compared to the selected protocols. This is due to the implementation of well organized F_{FS}. Our scheme mainly concerns reactive networks due to the requirement of time-sensitive applications and addresses the problem of higher energy consumption by utilizing depth difference between data forwarders. In AMCTD, nodes consume high energy as these transmit from far distance; however, in DBR, energy consumption increases

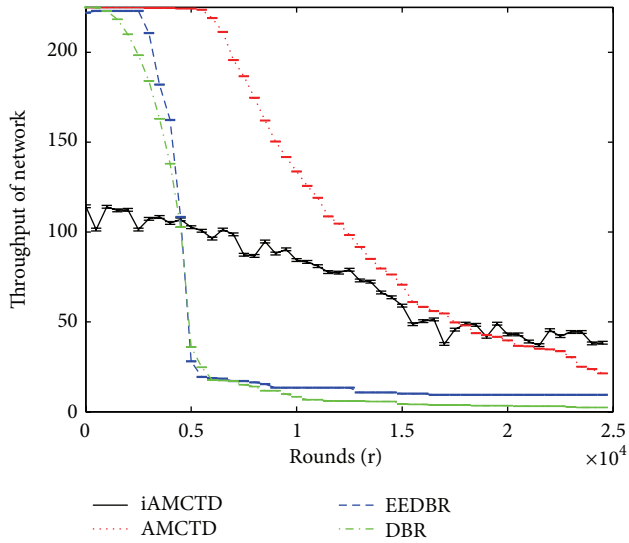

Figure 10: Comparison of network throughput in iAMCTD, AMCTD, EEDBR, and DBR.

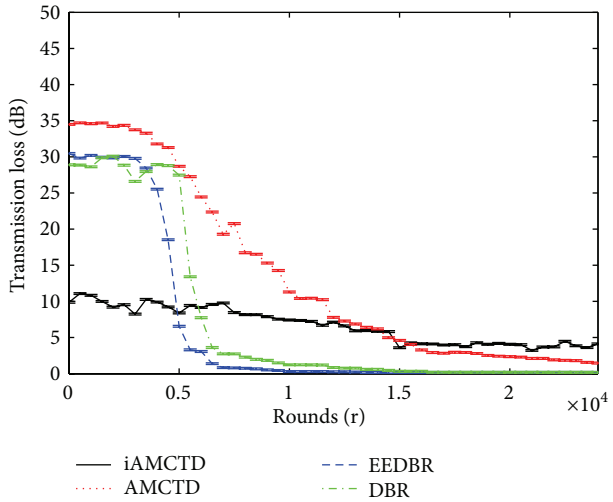

Figure 11: Comparison of transmission loss (dB) in iAMCTD, AMCTD, EEDBR, and DBR.

steadily as number of eligible neighbor drops off with the network density. In EEDBR, energy consumption is higher than other techniques due to frequent selection of high energy nodes, whereas, iAMCTD balances the energy consumption by proper forwarder selection and mobility patterns of courier nodes. In AMCTD, movements of courier nodes provide stability up to some extent to the remaining nodes; however, it is not sufficient for the whole network. In our system, there is higher energy consumption than the other protocols in the later rounds because of uniform network density. DBR shows better energy consumption management than EEDBR; however, it compromises on stability period. The adaptive mobility of courier nodes reduces distant forwarding

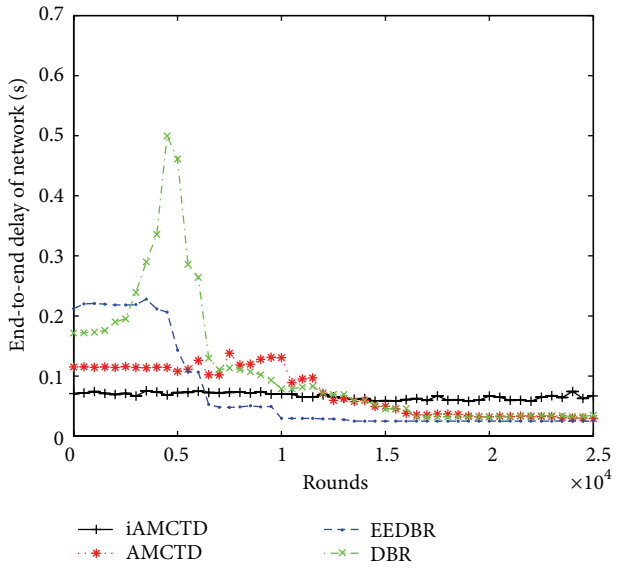

Figure 12: End-to-end delay in iAMCTD, AMCTD, EEDBR, and DBR.

in the later rounds and maintains the load on medium-depth nodes.

Figure 10 portrays throughput comparison of iAMCTD, AMCTD, EEDBR, and DBR. The throughput of iAMCTD demonstrates the amount of threshold-optimized data for responsive networks, as the proposed protocol avoids unnecessary data transmission, thereby leading to lower throughput. However, it ensures minimal transmission loss and end-to-end delay while delivering data. Previous schemes send unnecessary data along with high propagation losses; the throughput decreases sharply due to quick fall in network density. In our protocol, throughput steadily decreases due to maintenance of network density and low energy consumption.

The throughput of DBR and EEDBR declines very quickly, which is unsuitable for both delay-tolerant and delay-sensitive applications. AMCTD performs better than the previous schemes in instability period, but our scheme outperforms AMCTD due to less time lag in data delivery, thus validating its better performance in flooding-based protocols.

Figure 11 shows that transmission loss of the network in iAMCTD is much less than the previous techniques due to prioritization of SNR in calculations of F_{Fs}. Higher throughput in AMCTD is achieved in compromise of transmission loss as number of redundant transmissions between sender nodes and sink is increased. In DBR, there are preferences of distant transmissions; however, in EEDBR multiple transmissions increase transmission loss between sender node and the sink. We utilize thorp's attenuation model for underwater acoustics to calculate the transmission loss in packet forwarding between a source node and sink. It considers transmission frequency, bandwidth efficiency, and noise density which scrutinize the signal quality during data transmission.

EEDBR has higher loss than other techniques as it employs distant propagations as well as multiple forwarding. In DBR, the initial rounds show low losses due to high network density; however, as networks become sparse there is a sharp decrease in network performance causing high packet loss. In AMCTD, channel loss conditions are better than DBR and EEDBR, as the weight function computations consider both depth and residual energy of forwarding nodes; therefore, the propagations remain stable. In later rounds, the performance of AMCTD gradually decreases with the decrement in qualified forwarders; therefore, both the packet loss and delay increase.

In our proposed scheme, transmission loss is one of the key factors concerning the significance of data-sensitive responsive networks. The F_{Fs} computations and adaptive mobility of courier nodes cause almost constant path loss throughout the network lifetime. Variations in depth thresholds assist in selecting optimal data forwarder which increase the overall network throughput.

Figure 12 shows that end-to-end delay of network in iAMCTD is less than the previous techniques due to minimum forwarding distances between the nodes in both dense and sparse conditions. The delay in DBR suddenly increases because of sharp energy depletion of medium-depth nodes. However, in EEDBR higher delay is caused due to prioritization of residual energy. In DBR, delay is much higher in initial rounds due to distant data forwarding. It decreases gradually with the sparseness of the network, after about 5000 rounds. In EEDBR, delay increases whenever the network becomes scattered causing data forwarding at minimum distance. End-to-end delay in AMCTD is better than previous techniques as both threshold variations and weight functions perform global load balancing. In our technique, there is a minimum possible time lag due to consideration of signal quality and depth differences between sender and receiver nodes. It is more suitable for delay-sensitive applications specifically in on-demand routing.

5. Conclusion and Future Work

In this paper, we have proposed iAMCTD routing protocol to maximize the lifetime of reactive UWSNs. Amendments in F_{Fs} calculation technique enhance the network lifetime and reduce the transmission loss. Optimized mobility pattern of sink, in later rounds, minimizes end-to-end packet delay, especially for delay-sensitive applications and even in sparse conditions. Furthermore, variations in depth threshold increase the number of eligible neighbors thus minimize critical data loss in delay-sensitive applications.

As for future directions, we intend to design mathematical analysis of courier nodes' mobility. We are also interested in performing detailed analysis of the acoustic channel model to devise further routing metrics for optimal data forwarding.

Conflict of Interests

The authors declare that there is no conflict of interests regarding the publication of this paper.

References

[1] L. Freitag, M. Grund, S. Singh, J. Partan, P. Koski, and K. Ball, "The WHOI Micro-Modem: an acoustic communications and navigation system for multiple platforms," in *Proceedings of the MTS/IEEE (OCEANS '05)*, vol. 2, pp. 1086–1092, Washington, DC, USA, September 2005.

[2] S. Sanka and G. Konchady, "Communication between wireless sensor devices and gnu radio," http://wenku.baidu.com/view/64c8a0d289eb172ded63b7fd.html.

[3] A. F. Harris III and M. Zorzi, "Modeling the underwater acoustic channel in ns2," in *Proceedings of the 2nd International Conference on Performance Evaluation Methodologies and Tools (ICST '07)*, p. 18, Institut e for Computer Sciences, Social Informatics and Telecommunicat ions Engineering, 2007.

[4] I. F. Akyildiz, D. Pompili, and T. Melodia, "Underwater acoustic sensor networks: Research challenges," *Ad Hoc Networks*, vol. 3, no. 3, pp. 257–279, 2005.

[5] T. Hu and Y. Fei, "QELAR: a machine-learning-based adaptive routing protocol for energyefficient and lifetime-extende d underwater sensor networks," *IEEE Transactions on Mobile Computing*, vol. 9, no. 6, pp. 796–809, 2010.

[6] A. Wahid, S. Lee, and D. Kim, "A reliable and energy-efficient routing protocol for underwater wireless sensor networks," *International Journal of Communication Systems*, 2012.

[7] A. Wahid, S. Lee, H.-J. Jeong, and D. Kim, "Eedbr: energy-efficient depth-based routing protocol for underwater wireless sensor networks," in *Advanced Computer Science and Information Technology*, vol. 195 of *Communications in Computer and Information Science*, pp. 223–234, Springer, Berlin, Germany, 2011.

[8] Z. Zhou, Z. Peng, J.-H. Cui, and Z. Shi, "Efficient multipath communication for time-critical applications in underwater acoustic sensor networks," *IEEE/ACM Transactions on Networking*, vol. 19, no. 1, pp. 28–41, 2011.

[9] H. Yan, Z. J. Shi, and J.-H. Cui, "DBR: Depth-Based Routing for underwater sensor networks," in *NETWORKING 2008 Ad Hoc and Sensor Networks, Wireless Networks, Next Generation Internet*, vol. 4982 of *Lecture Notes in Computer Science*, pp. 72–86, Springer, 2008.

[10] M. Ayaz, A. Abdullah, I. Faye, and Y. Batira, "An efficient dynamic addressing based routing p rotocol for underwater wireless sensor networks," *Computer Communications*, vol. 35, no. 4, pp. 475–486, 2012.

[11] X. Liu, X. Gong, and Y. Zheng, "Reliable cooperative communications based on random ne twork coding in multi-hop relay WSNs," *IEEE Sensors Journal*, vol. 14, no. 8, pp. 2514–2523, 2014.

[12] J. Rezazadeh, M. Moradi, A. Ismail, and E. Dutkiewicz, "Superior path planning mechanism for mobile beacon-assisted localization in wireless sensor networks," *IEEE Sensors Journal*, 2014.

[13] J. Zou, S. Gundry, J. Kusyk, M. Ü. Uyar, and C. S. Sahin, "3D genetic algorithms for underwater sensor networks," *International Journal of Ad Hoc and Ubiquitous Computing*, vol. 13, no. 1, pp. 10–22, 2013.

[14] C.-M. Chao and M.-W. Lu, "Energyefficient transmissions for bursty traffic in underwater sensor networks," *International Journal of Ad Hoc and Ubiquitous Computing*, vol. 13, no. 1, p. 19, 2013.

[15] W. Liao and C. Huang, "SF-MAC: a spatially fair MAC protocol for underwater acoustic sensor networks," *IEEE Sensors Journal*, vol. 12, no. 6, pp. 1686–1694, 2012.

[16] M. Mirsadeghi and A. Mahani, "Energy efficient fast predictor for wsn-based target tracking," *Annals of Telecommunications*, 2014.

[17] B. Borowski and D. Duchamp, "Measurement-based underwater acoustic physical layer simulation," in *Proceedings of the MTS/IEEE Seattle (OCEANS '10)*, pp. 1–8, IEEE, Seattle, Wash, USA, September 2010.

[18] M. Stojanovic, "On the relationship between capacity and distance in an underwater acoustic communication channel," *ACM SIGMOBILE Mobile Computing and Communications Review*, vol. 11, no. 4, p. 3443, 2007.

[19] B. S. Sharif, J. Neasham, O. R. Hinton, and A. E. Adams, "A computationally efficient doppler compensation system for underwater acoustic communications," *IEEE Journal of Oceanic Engineering*, vol. 25, no. 1, pp. 52–61, 2000.

[20] S. Gopi, G. Kannan, D. Chander, U. B. Desai, and S. N. Merchant, "PULRP: path unaware layered routing protocol for underwater sensor networks," in *Proceedings of the IEEE International Conference on Communications (ICC '08)*, pp. 3141–3145, IEEE, May 2008.

[21] M. Jafri, S. Ahmed, N. Javaid, Z. Ahmad, and R. Qureshi, "AMCTD: adaptive mobility of courier nodes in threshold-optimized DBR protocol for underwater wireless sensor networks," in *Proceedings of the 8th IEEE International Conference on Broadband and Wireless Computing, Communication and Applications (BWCCA '13)*, Compiegne, France, October 2013.

[22] S. Ibrahim, J. Cui, and R. Ammar, "Surface-level gateway deployment for underwater sensor networks," in *Proceedings of the IEEE Military Communications Conference (MILCOM '07)*, pp. 1–7, Orlando, Fla, USA, October 2007.

[23] W. K. Seah and H.-X. Tan, "Multipath virtual sink architecture for underwater sensor networks," in *Proceedings of the Asia Pacific Conference (OCEANS '06)*, pp. 1–6, IEEE, Singapore, May 2007.

[24] Z. Zhou, J.-H. Cui, and S. Zhou, "Localization for large-scale underwater sensor networks," in *NETWORKING 2007: Ad Hoc and Sensor Networks, Wireless Networks, Next Generation Internet*, vol. 4479 of *Lecture Notes in Computer Science*, pp. 108–119, Springer, New York, NY, USA, 2007.

[25] R. J. Urick, *Principles of Underwater Sound*, McGraw-Hill Ryerson, 1983.

[26] J. Wills, W. Ye, and J. Heidemann, "Low-power acoustic modem for dense underwater sensor networks," in *Proceedings of the 1st ACM International Workshop on Underwater Networks (WUWNet '06)*, pp. 79–85, ACM, September 2006.

[27] D. Shin and D. Kim, "A dynamic NAV determination protocol in 802.11 based underwater networks," in *Proceeding of the IEEE International Symposium on Wireless Communication Systems (ISWCS '08)*, pp. 401–405, Reykjavik, Iceland, October 2008.